ISSN: 0974-5823 Vol. 6 No. 3 December, 2021

International Journal of Mechanical Engineering

Synthesis, structural elucidation, and biological activities of biomaterial containing biologically active ligand derived from Schiff base

C.Justin Dhanaraj [a] & M. Jebapriya [b*]

[a] Department of Chemistry, University College of Engineering, Anna University,Tirunelveli Region, Konam, Nagercoil-629 004,Tamil Nadu,India

[b]Department of Chemistry, Mar Ephraem College of Engineering and Technology, Elavuvialai, Marthandam-629 171, Tamil Nadu,India

Abstract

Metal ion activity as biomaterials have prompted the evolution of metal-based therapeutics and so novel 4-aminoantipyrine and benzoin based Co(II), Ni(II), Cu(II) and Zn(II) complexes were synthesized and characterized using different physicochemical techniques, incorporating elemental analysis, conductance studies, Fourier transform infrared spectroscopy (FTIR), ultraviolet-visible (UV-Vis) spectrophotometry, nuclear magnetic resonance spectrophotometry (^{1}H NMR & ^{13}C NMR), magnetic susceptibility and mass spectrometry. Octahedral geometry has been proposed to Co(II), Ni(II) and Zn(II) complexes, and Cu(II) complex possess distorted octahedral geometry. Electrochemical behaviour of the synthesised Cu(II) compounds were evaluated employing cyclic voltammetry Thermal properties of complexes were established by thermo gravimetric analysis. *In vitro* biological activities such as antimicrobial, DNA cleavage, SOD and anticancer activities of the complexes were evaluated. Antimicrobial activities of complexes have been determined on Gram-positive (*Bacillus subtilis and Staphylococcus aureus*), Gram- negative (*Escherichia coli and Pseudomonas aeruginosa*) bacteria and on the fungal species *Aspergillus niger*, *Aspergillus flavus* and *Candida albicans.* Nuclease activity of ligand and its complexes were determined by gel electrophoresis on CT DNA. Synthesised compounds were screened for antioxidant activity using NBT method and *in vitro* anticancer activities were analysed against Liver Bilobular cancerous (LBir2754) cell line.

Key words: Antipyrine, metal complexes, Antimicrobial, SOD and Anticancer

Introduction

Positively charged metal centers are indulged to bind to biomolecules which are negatively charged. Thus, the pharmaceutical application of metal complexes has outstanding potential [1]. Schiff base and their metal complexes are immensely well known because of their miscellaneous chelating capabilities [2]. 4-Aminoantipyrine is a pain reducing pyrazole derivative with free amino group that can form Schiff base derivatives with aldehydes and ketones [3]. Benzoin is an α- Hydroxy ketone which is useful in the synthesis of Schiff base ligands that possess well known application in medicinal and industrial field [4]. Schiff bases are been reviewed for their magnificent biological activities and previous works carried out in last decades have identified the ability of Schiff bases and their complexes to possess various bioactive effects [5]. Schiff bases have the ability to form complexes and due to its pharmacological properties, they are revealed to be the promising leads for designing more desirable antimicrobial agents [6]. Schiff bases and their complexes are found to possess the ability to combine with lipophilic layer to increase the membrane permeability of biological applications [7,8]. Several microorganisms have been described with antibiotic resistances and it is the necessity of time to develop new therapeutic alternatives [9, 10]. Thus we decided to report on the synthesis, characterization and the biological activity of metal complexes of Schiff base derived from 4-aminoantipyrine and benzoin.

Experimental

2.1. Materials

Materials of AnalaR grade were utilized in the experimental process. 4-Aminoantpyrine and benzoin was purchased from Himedia. The Liver Bilobular cancerous LBir2754 cell was collected from National Centre for Cell Science (NCCS), Pune. Co(II), Ni(II), Cu(II), and Zn(II)acetates obtained from Merck were utilised as such. MeOH, C_2H_5OH, $CHCl_3$, CH_3COOH and diethyl ether were purchased from the Sd fine Chem Ltd. Reagents and solvents of analytical grade were used, and so they required no further purification.

2.2. Synthesis of Schiff Base Ligand (L)

To methanolic solution of 4-AAP (0.002 mol), warm methanolic solution of benzoin (0.002 mol) was added dropwise. After the addition of benzoin, the clear solution obtained was stirred with heating at about 75-80° C for 4-5 hrs. The resultant solution was transfered into cold water and the obtained solid product is filtered and washed with petroleum ether and dried. The crude sample is recrystallized from hot aqueous methanol (**Scheme - I**).

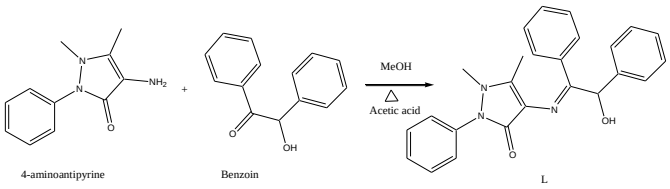

2.3. Synthesis of complexes

A mixture of L (2 mmol) in 25 mL of methanol was taken in a 100 mL round bottomed flask. A solution of metal(II) acetate (2 mmol) in methanol was added. The mixture was stirred vigorously at 60^0 C for 10 h. The contents of the reaction were cooled to room temperature. The precipitate formed was filtered off, washed appropriately over anhydrous $CaCl_2$ (**Scheme – II)**.

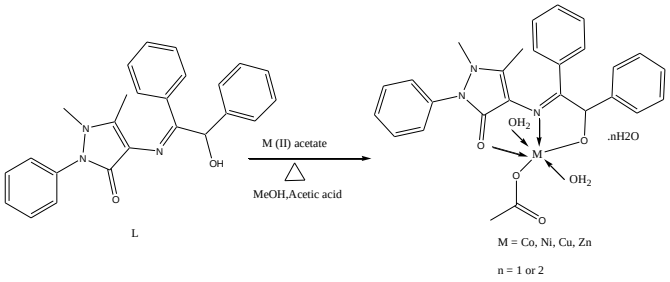

2.4. Physical Measurements

Perkin-Elmer elemental analyzer analyzed the elements present and metal contents were found by EDTA titrations [11]. Conductance was recorded on Coronation digital conductivity meter. GC mass spectra were determined on JMS-T 100LC mass spectrometer in m/z range 50-1200. ^{1}H and ^{13}C NMR spectra in $CDCl_3$ were obtained on bruker FT–NMR spectrometer. FTIR spectra in 4000-400 cm^{-1} region were noted using KBr on JASCO FT/IR-410 spectrometer. UV-Vis spectra were recorded with Perkin Elmer Lambda-25 UV-Vis spectrometer. Magnetic measurements at room temperature were determined on Guoy balance. Thermal analysis performed on SDT Q 600/V8.3 build 101 thermal analyzer at 20 ^{0}C/min heating rate using nitrogen atmosphere. Electrochemical analysis was performed using electrochemical workstation, CHI 650C.

2.5. Antimcrobial activity

Antimicrobial properties of L and its mixed ligand complexes were determined *in vitro* against fungal species, *A. niger*, *A. flavus*, and *C. albicans* and bacterial species *E. coli*, *B. subtilis*, *P. aeruginosa*, and *S. aureus*; by disc diffusion technique. Amikacin, ofloxacin, and ciprofloxacin acted as controls for antibacterial analysis and control for antifungal analysis is nystatin. Test species were grown in petri plates on agar medium. The compounds in DMSO were placed in filter paper disc kept on priorly seeded plates and set at 37 ^{0}C. Inhibition zone is calculated after 24 hours for antibacterial and 72 hours for antifungal analysis. Minimum inhibitory concentration (MIC) was analysed using 'serial dilution method' [12].

2.6. DNA cleavage activity

CT DNA in buffer solution (5 mmol L^{-1} Tris–HCl / 50 mmolL^{-1} NaCl buffer (pH 7.2) recorded UV absorbance ratio 1.89:1 at 260 and 280 nm, indicating protein contamination free CT DNA. DNA cleavage ability was determined employing agarose gel electrophoresis [13]. CT DNA (0.3 µg) in 5 mmol L^{-1} Tris–HCl/50 mmol L^{-1} NaCl buffer (pH 7.2), with mixed ligand complexes was set at 37 ^{0}C for 2 hours and treated using buffer (2 µL) consisting 25% bromophenol blue, 0.25% xylene cyanol and 30 % glycerol. Electrophoresis was conducted for 2 hours at 50 V in Tris–acetate–EDTA (TAE) buffer (pH 8.0) and ethidium bromide stained gel was photographed under UV light 5 min after the process.

2.7. SOD activity

In vitro SOD activity was determined with alkaline DMSO as superoxide radical (O_2^-) source and nitrobluetetrazolium (NBT) as scavenger [14]. 400 millilitres of sample was mixed with 2.1 millilitres of 0.2 M K_3PO_4 buffer (pH 8.6) and 1 millilitre of 56 mM NBT. Samples were ice cooled for 15 min and 1.5 millilitres alkaline DMSO was added and agitated well. Absorbance was recorded at 540 nm.

2.8. *In vitro* anticancer activity

Human Liver Bilobular cancerous LBir2754 cells were grown in EMEM and it contains 10% FBS. The cells were sustained at required conditions (37 ^{0}C, 5% CO_2, 95% air, and 100% relative humidity). To create cell suspension, monolayer cells were separated using trypsin-EDTA and viable cell count was measured using hemocytometer. It is diluted using medium consisting 5% FBS to get $1x10^5$ cells/mL as final density. 100 microliters of suspension per well was seeded on well plates with 10,000 cells/well plating density. For cell attachment, plates were incubated at required conditions and cell specimens were treated for 24 h. Initially, they were dissolved in DMSO for stock preparation (200 mM) and preserved in frozen condition. Aliquot was thawed for sample addition and diluted to required concentrations. Five concentrations of sample were prepared and 100 µL of these samples were mixed with wells containing 100 µL medium and incubated for extra 48 hours at required conditions [15].

MTT is yellow coloured tetrazolium salt soluble in water. Succinate dehydrogenase enzyme converts MTT into insoluble purple formazan. Quantity of formazan formed is proportionally equivalent to viable cell count. 15 µL MTT (5 mg/mL) was treated to wells after 48 hours of incubation in PBS. MTT was then flicked off and 100 µL DMSO is used to dissolve formazan crystals and at 570 nm, its absorbance was measured [16]. Using the following formula, percent cell inhibition was calculated.

% cell inhibition = 100 - Abs (sample)/Abs (control) x100

The nonlinear regression graph was recorded using Graph Pad Prism software IC_{50} was calculated.

3. Results and discussion

3.1. Characterization of Schiff Base Ligand (L)

Synthesized ligand (L) is stable, and dissolves in common organic solvents. Data of elemental analysis (Table 1) is in accordance with that of the determined value of suggested formula. The general formula of the ligand is $C_{25}H_{23}N_3O_2$. Molecular weight of the ligand calculated is 397.18.

FTIR spectrum of L (Figure –S1) exhibits a band at 1677 cm^{-1} assigned to the stretching frequency of the carbonyl moiety

present. L displays a band at 1593cm^{-1} is attributable to CH=N group. Two bands present at 1205 cm^{-1}and 1067 cm^{-1} is because of the stretching frequency of C=O and C=N respectively. A wide peak present around 3414 cm^{-1} is owing to the OH group of L.

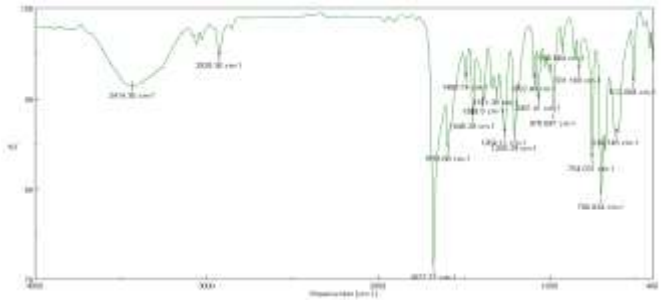

Figure-S1: FTIR spectrum of L

^{1}H-NMR of L (Figure-S2) exhibits two singlets at δ 1.25 and δ 3.12 ppm attributed to the two methyl groups (C-CH_3 and N-CH_3) present in the 4-AAP moiety. Signals at δ 2.35 and δ 5.95 are due to protons (C-H and O-H) of keto group in benzoin moiety. The peaks at δ 7.23-8.15 ppm have been attributed to chemical shifts of aromatic protons of phenyl rings present in L. ^{13}C-NMR spectrum, displays peak of carbons present in CH=N groups at 168 ppm (Figure –S3). Carbon atoms present in aromatic ring gives peak at 115-139 ppm range. Two methyl carbon atoms of 4- AAP moiety appears at 16 and 35 ppm. The carbon present near carbonyl group displays a band at 162 ppm. Carbon near to OH group shows a peak at 151 ppm.

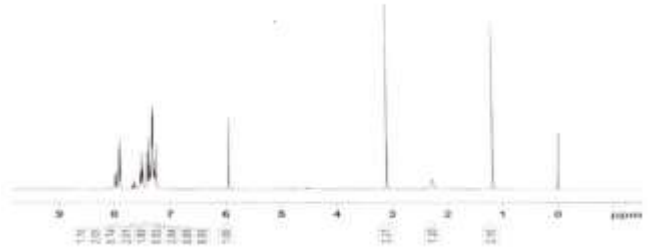

Figure-S2: ^{1}HNMR spectrum of L

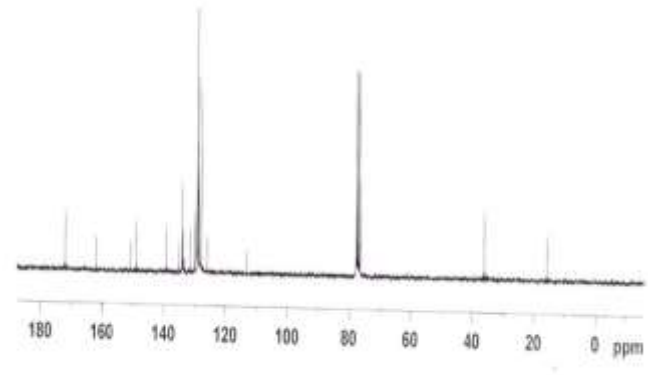

Figure-S3: ^{13}CNMR spectrum of L

The recorded GC mass spectrum of L sows the molecular ion peak at m/z = 398 [M+1 (100 %)], (Figure –S4) which corresponds to that of the formula weight of L. The base peak and the molecular ion peak are same in this system. The mass peaks at 309, 284, 214, 151 are related to the mass of the fragments formed from the ligand. The mass fragmentation representation is shown in figure - 1.

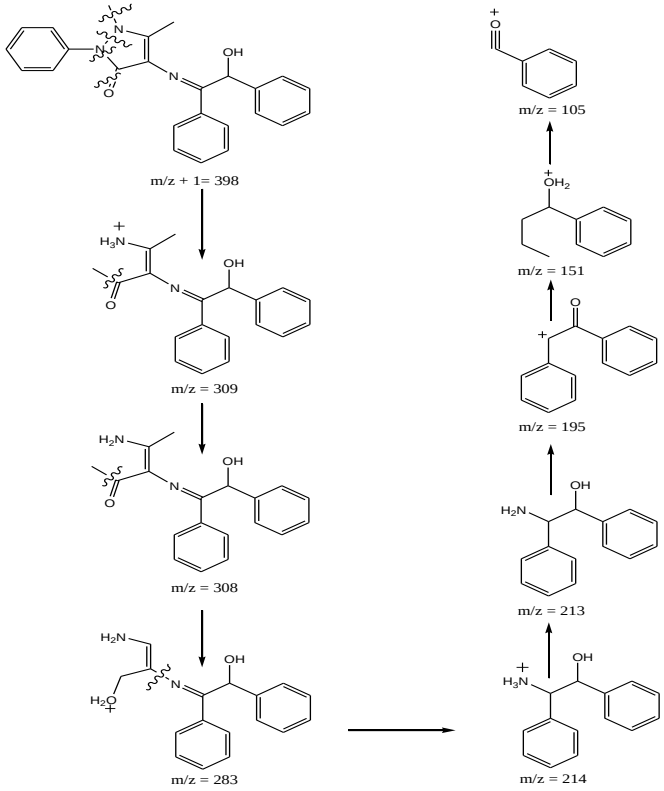

Figure-1: Mass spectral fragmentation representation of **L**

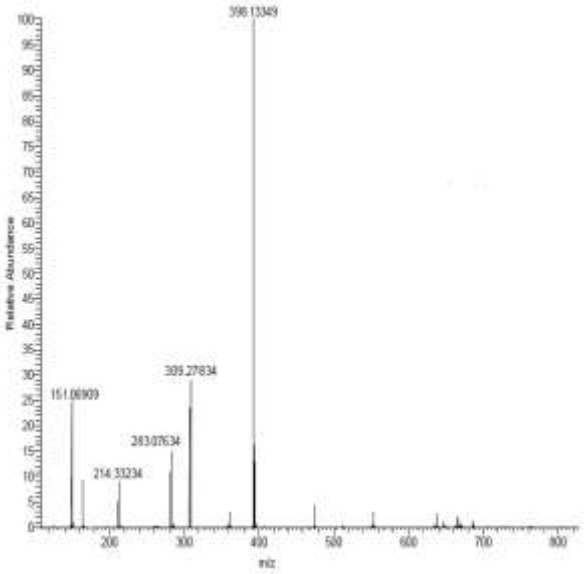

Figure-S4: GC mass spectrum of L

UV visisble spectrum of L shows (Figure -S5) absorption bands at 252, 395 nm, attributed to π-π* and n-π* transitions of the CH=N chromophore in L. The double bond present in the CH=N and carbonyl moiety are the reason for the n-π*

transitions.π-π* transitions is mainly due to the aromatic group of the ligand.

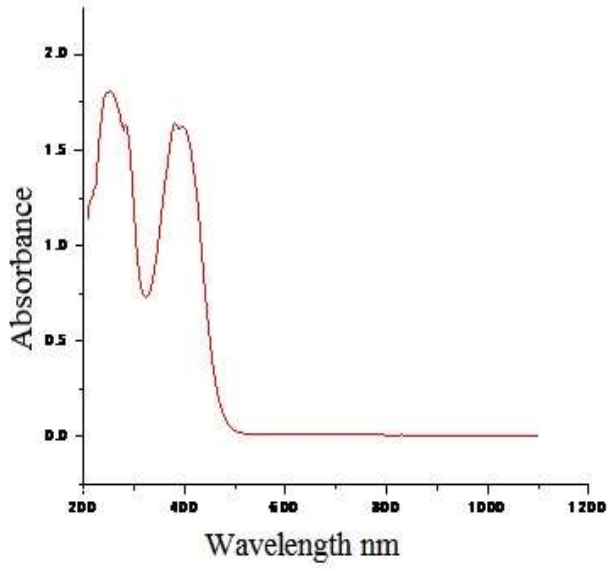

Figure-S5: UV visible spectrum of L

Table-1: Analytical data of L and its metal complexes

Compound	M.W	Elemental analysis Found (calcd) %				Λc (Ohm^{-1} cm^2mol^{-1})	λ_{max} (nm)	μ_{eff} (B.M)
		C	H	N	M			
L	397.47	75.76 (75.54)	5.99 (5.83)	10.28 (10.57)	-		252, 393	-
[CoLOAc]	569.48	56.71 (57.04)	5.98 (5.50)	7.65 (7.39)	9.96 (10.37)	08	258, 398,650	4.90
[NiLOAc]	586.26	54.99 (55.31)	5.93 (5.67)	6.94 (7.17)	10.43 (10.01)	11	260,400, 600, 1000	3.10
[CuLOAc]	591.11	54.45 (54.86)	5.21 (5.63)	7.53 (7.11)	10.39 (10.75)	10	262,400, 700	1.90
[ZnLOAc]	574.94	55.95 (56.30)	5.71 (5.43)	7.69 (7.31)	10.97 (11.37)	07	265, 398	Dia

3.2. Characterization of Metal Schiff Base Complexes

The findings represent details on the ratio of metal to ligand, and are found to be 1:1. The general formula for the composition of complex is $[ML(CH_3COO)(H_2O)_2]$. nH_2O, where M is the metal ion Co(II), Ni(II), Cu(II), Zn(II), L is the synthesized Schiff base L and n may be 1 or 2. The complexes are found to dissolve in methanol, ethanol, $CHCl_3$, DMF and DMSO. The low molar conductance values expose their non-electrolytic nature.

3.3 FTIR Spectra

Table: 2 provides FTIR spectral information of the complexes. FTIR bands (Figure- 2) at $1677cm^{-1}$ of the carbonyl group of free ligand is shifted to low frequency range of ~1658-1661 in complexes confirms the coordination with carbonyl oxygen atom. The band at 1593 cm^{-1} of the CH=N group of free ligand is shifted to low frequency range of ~1560-1591 cm^{-1} in the complexes confirms the coordination of the metal ion with CH=N nitrogen. Broad band present in~3400 cm^{-1} is assigned the stretching frequency of coordinated and lattice water molecules present. A band at 1205 cm^{-1} for C-O stretching frequency present in the free ligand shifted to high frequency range of ~1213-1217 cm^{-1} in the complexes gave some evidence to the coordination of OH group with the metal atom. Spectral bands around 549-550 cm^{-1} may be generally because of the formation of M-O bonds [17].

Table-2: FTIR spectral data of metal complexes of L

Compound	$\nu_{azo.}$ (C=O)	$\nu_{azo.}$ (C=N)	ν (C-O)	ν (OH)	N (H_2O)	N (M-O)
L	1677	1593	1205	3414(b)	-	-
[CoLOAc]	1661	1560	1215	-	3431(b)	549
[NiLOAc]	1658	1590	1217	-	3438(b)	549
[CuLOAc]	1661	1592	1213	-	3430(b)	550
[ZnLOAc]	1661	1591	1215	-	3432(b)	549

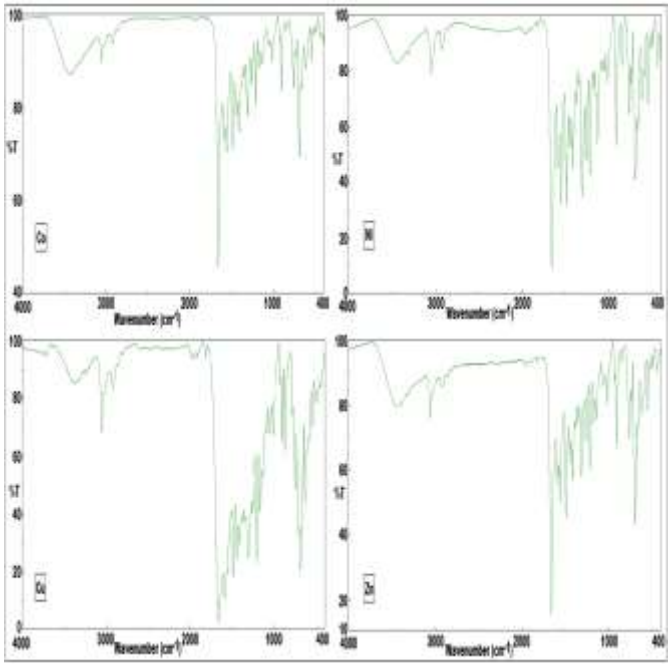

Figure-2: FTIR spectra of metal chelates with L

3.4 GC mass spectra

GC mass spectra of the Co(II), Ni(II), Cu(II), and Zn(II) complexes show (Figure -3) molecular ion peaks at m/z 568 (M+, 50%), 586 (M+, 43 %), 591 (M+, 36%), and 574 (M+,21%) and that is in accordance with those of the calculated formula weight.

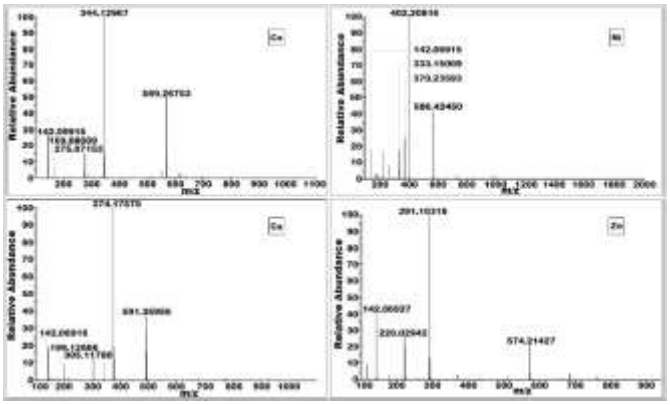

Figure-3: GC mass spectra of metal chelates with L

3.5 UV-visible spectra and magnetic properties

UV visible spectral bands present in at 252 and 395 nm suggesting the transitions π-π* and n-π* of azomethine chromophore of the free ligand are moved to ~258-265 and ~398-400 nm. It also proves the coordination with the M(II) ion. The UV spectrum of Co(II) complex (Figure - 4) shows band around ~650 nm region, which is assignable to $^4T_1g(F)\rightarrow{}^4A_2g(F)$ and $^4T_1g(F)\rightarrow{}^4T_2g(F)$ transitions in octahedral environment [18]. For the Co(II) complex, magnetic susceptibility value found is 4.90 BM. The magnetic susceptibility range apparent for octahedral complexes of Co(II) is usually about 4.3-5.2 BM. The octahedral geometry of the Co(II) complex was therefore inferred by this result. The electronic spectrum shows three distinct bands assigned to to $^3A_2g(F)\rightarrow{}^3T_2g(F)$, $^3A_2g(F)\rightarrow{}^3T_1g(F)$, and $^3A_2g(F)\rightarrow{}^3T_1g(P)$ transitions in the region of ~1000, 600, and 400 nm for the Ni(II) complex. This is an indication of octahedral geometry of the Ni(II) ion[19]. The Ni(II) complex magnetic moment is estimated to be 3.10 BM, which coincides with the standard range for Ni(II) (2.9-3.3 BM) [20]. The Cu(II) complex UV shows a wide band in the region of ~700 nm that can be given to the transition of $^2Eg\text{-}^2T_2g$, indicating that the copper complex has distorted octahedral geometry. The Jahn-Teller effect will be more pronounced when the odd number of electrons reaches the Eg orbitals of an octahedral Cu complex. The calculated magnetic moment value is 1.90 BM for the Cu(II) complex and that is agreement octahedral Cu(II) complexes. d-d transformation is not shown by diamagnetic Zn(II) complex.

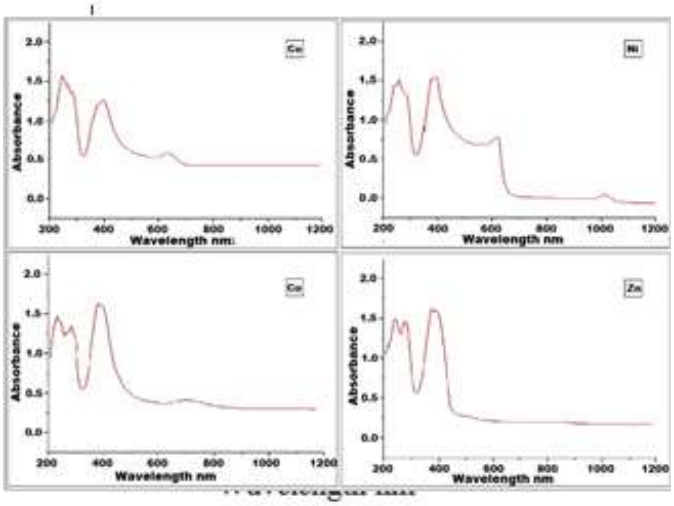

Figure-4: UV visible spectra of metal chelates with L

3.6 Electrochemical Studies

The recorded electrochemical behavior of Cu(II) complex is shown in Figure - 5. As we see the Cu(II) complex's electrochemical properties, it gives a pair of 0.05 mV and 0.56 mV cathodic and anodic peak potentials, reflecting the Cu(II)/Cu(I) couple. The peak-to-peak separation value of (ΔEp = 0.61 mV) indicates quasi-reversible one-electron transfer mechanism. Electrochemical analysis data of Cu(II) complex is tabulated in Table-3.

Table-3: Electrochemical analysis data of Cu(II) complex of L

Complex	E_{pc}(V)	E_{pa}(V)	ΔEp (V)	i_{pa}(A)	i_{pc}(A)	i_{pa}/i_{pc}(A)
[CoLOAc]	-0.05	0.56	0.61	0.89	-0.93	-0.82

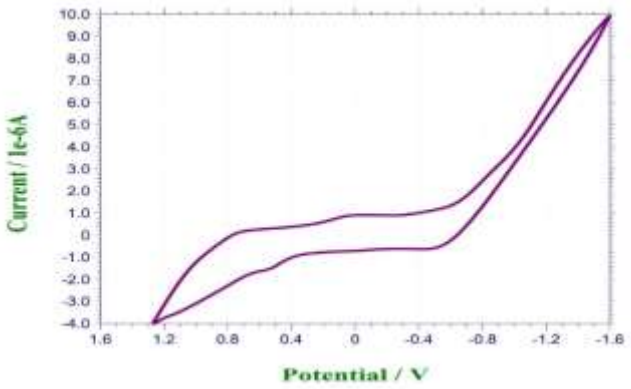

Figure-5: Cyclic voltammogram of Cu(II) chelate of L

3.7 Thermo gravimetric analysis

The thermo gravimetric analysis data of the Schiff base metal (II) complexes are tabulated in Table- 4. Co(II) complex shows a mild weight loss of 3.40% (calculated - 3.16 %) in 60-100 ^{0}C temperature range(Figure -6). This is due to the loss of one water molecule trapped in the lattice. Second phase, the complex shows a break down at higher temperature range from 170 to 250 ^{0}C and a loss in weight of 6.00 % (calculated 6.34 %) which coincides with the loss of two coordinated water molecules from the complex. The next decomposition step shows a loss in weight of 77.70 % (calculated - 77.30 %) at a temperature range 260-580 ^{0}C which indicates the complete removal of the ligand. Above this temperature, a flat thermal curve seen because of metal residue formation. Nil(II) complex shows a loss in weight of 6.00 % (calculated 6.15 %) in 70-110 ^{0}C temperature range indicating the removal of two lattice water molecules. The curve shows a loss in weight of 6.10 % at 160-240 ^{0}C temperature range (calculated value is 6.15 %). This is indicated by the elimination of two coordinated water molecule from the Ni(II) complex. Third weight loss of 75.40 % (calculated 74.93 %) in 270-600 ^{0}C due to the removal of coordinated ligand moiety. A straight curve is seen because of metal residue formation. Cu(II) complex shows a

decomposition curve 70-120 ^{0}C temperature range causing a loss in weight of 6.40 % (calculated 6.10 %) which is because of the removal of two lattice water molecule present in the complex. The second decomposition shows a loss in weight of 5.90 % (calculated - 6.10%) in 170-250 ^{0}C is because of the removal of two coordinated water molecules from the complex [21]. The third weight loss 74.50 % in 260-570 represents the complete removal of the organic ligand moiety. The calculated value was 74.33 % for organic ligand moiety. Above 570 ^{0}C, a flat curve is seen because of the formation of metal residue. Zn(II) complex shows a loss in weight of 3.80 % (calculated 3.14 %) in 60-90 ^{0}C temperature range representing the removal of one lattice water molecule from the complex. The second decomposition stage of the metal complex is in 170-240 ^{0}C range of temperature showing a weight loss of 6.20 % (calculated 6.28 %) indicating the exclusion of two coordinated water molecules. The next decomposition stage shows a weight loss of 76.00 % (calculated -77.41 %) in 260-550 ^{0}C temperature range. This step represents the complete removal of ligand. Above this temperature, a straight line is seen because of the formation of final metal residue.

Table-4: Thermo gravimetric analysis data of metal complexes of L

Complex	Temperature range T (ºC)	% Weight loss Obs.(calcd)	Process
[CoLOAc]	60-100 170-250 260-580 >580	3.40(3.16) 6.00(6.34) 77.70(77.30) 12.90(13.20)	-H_2O(Lattice) -2H_2O(Coord.) loss of organic moiety Co residue
[NiLOAc]	70-110 160-240 270-600 >600	6.00(6.15) 6.10(6.15) 75.40(74.93) 12.50(12.77)	-2H_2O(Lattice) -2H_2O(Coord.) loss of organic moiety Ni residue
[CuLOAc]	70-120 170-250 260-570 >570	6.40(6.10) 5.90(6.10) 74.50(74.33) 13.20(13.47)	-2H_2O(Lattice) -2H_2O(Coord.) loss of organic moiety Cu residue
[ZnLOAc]	60-90 170-240 260-550 >550	3.80(3.14) 6.20(6.28) 76.00(77.41) 14.00(14.20)	-H_2O(Lattice) -2H_2O(Coord.) loss of organic moiety Zn residue

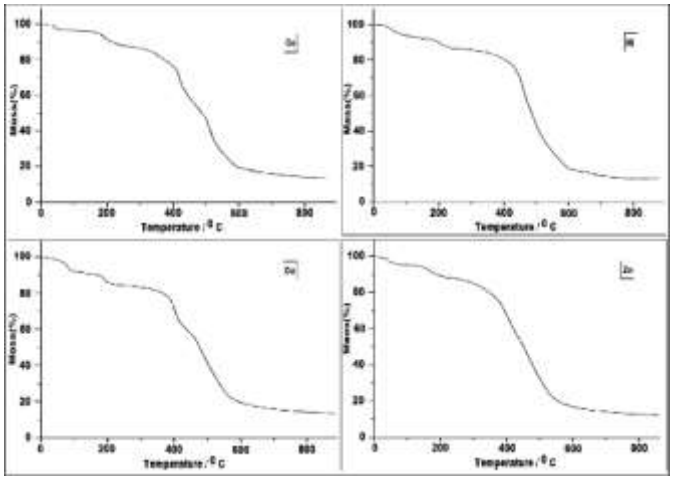

Figure-6: Thermograms of metal chelates of L

On the basis of all the spectral and analytical studies, the anticipated structure of the metal complex is given in the Figure – 7

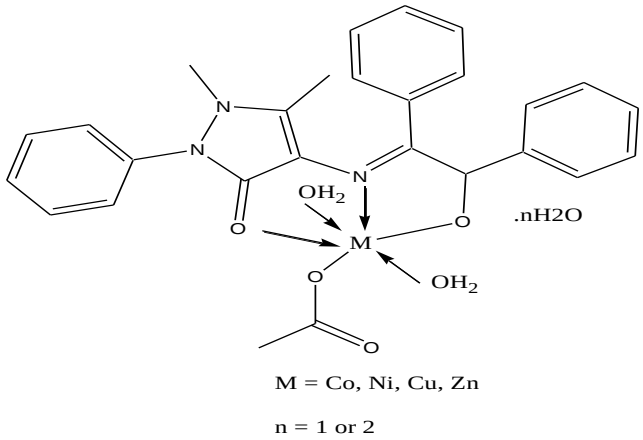

Figure-7 : Proposed structure of metal chelates of L

4. Biological Studies

4.1 Antimicrobial activity

The results of antibacterial and antifungal activity are summarized in Table-5. Under identical conditions, the experiment was replicated three times. Amikacin and ciprofloxacin were utilized as positive control and DMSO acted as a negative control for antibacterial studies. Nystatin was used as a standard for antifungal studies. Bacteria possess better activity and the fungi shows lower activity.

Table-5: In vitro antimicrobial activity of L and its complexes

Compound	Bacterial species				Fungal species		
	E. coli	***B. subtilis***	***P. aeruginosa***	***S. aureus***	***A. niger***	***A. flavus***	***C. albicans***
L	45	>100	>100	>100	95	>100	>100
[CoLOAc]	30	81	19	64	48	23	31
[NiLOAc]	23	38	20	53	41	28	36
[CuLOAc]	05	10	21	20	08	18	09
[ZnLOAc]	72	80	>100	>100	69	>100	90
Amikacin[a]	05	05	04	05	-	-	-

Ciprofloxacin[a]	05	05	05	05	-	-	-
Nystatin[a]	-	-	-	-	06	06	05

The Schiff base copper complex exhibits higher activity against bacterial and fungal species than the other metal complexes. A remarkable activity is shown by the Copper (II) complex, especially against *E. coli*. The antimicrobial activity of the metal complexes is greater than that of the free ligand; which means that the activity of the ligand is strengthened effectively by the complexation of the metal. On the basis of the principle and the chelation theory and Overtone concept, this can be explained. Chelation helps to make a more effective and potent antibacterial and antifungal agent for the Schiff base ligand[22].

4.2 DNA cleavage activity

Gel electrophoresis examination using CT DNA in the presence of an oxidant was performed with L. Cu(II) and Zn(II) complexes cleave the DNA completely, but the Co(II),

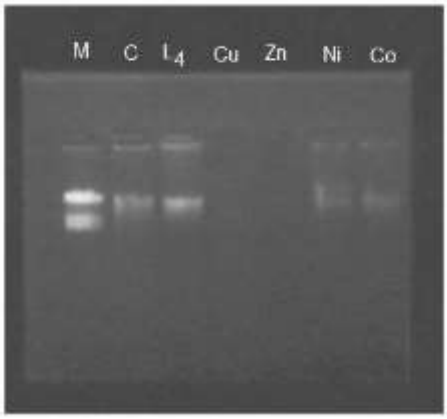

Ni(II) as well as L shows partial cleavage of DNA (Figure-8).

Figure-8: DNA cleavage image of L and its metal chelates (M- Marker, C- Control)

4.3 SOD activity

Table-6 gives the SOD activity readings (IC_{50}) of the Schiff base ligand and its metal(II) complexes. Compared to that of the native enzyme, the activity effects of the ligand and its metal(II) complexes are mild. The Copper(II) complex is showing better behaviour among the metal complexes. Schiff base metal complexes or any other organic or inorganic compounds in which single electron oxidation follows the reduction of metal ions or the formation of SOD complexes, which can be further reduced by any other superoxide ion to peroxide, are known to be SOD active species .To find the mechanism of this SOD active action, UV-Visible spectrum of the compounds were taken. In both the presence and the absence of alkaline DMSO, the spectrum was observed (O_2^- source is alkaline DMSO). The peaks were found to be obscured when alkaline DMSO containing the buffer was present (pH -8.6). The same peaks returned to their initial location when we used NBT (O_2^- scavenger).

Table-6: SOD activity data of L and its complexes

Compounds	IC_{50} (µM)
L	72.6
[CoLOAc]	36.7
[NiLOAc]	41.3
[CuLOAc]	14.2
[ZnLOAc]	48.8
Native SOD	5

4.4 Anticancer activity

In order to analyze the anticancer effects of L and its chelates, we used human liver bilobular cancerous LBir2754 cells at the concentrations of 6.25, 12.5, 25, 50, and 100 µM for 48h (Figure -9). The control untreated cells. The MTT assay analysed cell growth inhibition and the findings showed that the complexes and the ligand had an inhibitory effect on the dose-dependent proliferation of LBir2754 cells (Table-7). Among them, compared to other metal complexes and the free Sciff base ligand, the Copper(II) complex demonstrated the most potent inhibitory effect on the growth of both cells. The potential mechanism could be the hydrogen bonding of metal complexes with the cell constituents and the decrease in cell activity leading to cancer cell death [23,24].

Table-7: IC_{50} values of $L_4$and its complexes

Compound	IC_{50} (µM)
L	95.6
[CoLOAc]	71.2
[NiLOAc]	59.4
[CuLOAc]	28.7
[ZnLOAc]	45.9

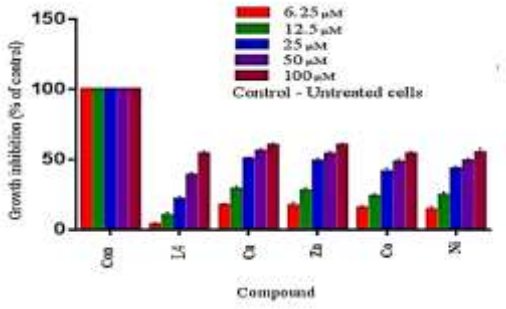

Figure-9: Anticancer activities of L and its complexes.

Conclusion:

The ligand **L** was formed by the condensation of 4-AAP with benzoin. Cobalt, nickel, copper and zinc coordination chelates of **L** were synthesized. They were analyzed by spectral and analytical techniques.1:1 stoichiometry for the metal and **L**

has been observed for all the synthesized compounds. All the coordination complexes of **L** show non electrolytic behaviour. NMR result confirms the formation of Sciff base ligand. The GC mass peaks at 309, 284, 214, 151 are related to the mass of the fragments formed from the ligand. Tridentate coordination of **L** with the metal ion coordinating through azomethine nitrogen, pyrazolone oxygen and through deprotonation of -OH group has been revealed from FTIR spectral analysis. UV-Vis spectral results and magnetic moment values confirm that, octahedral structure has been exhibited by Co(II), Ni(II) and Zn(II) chelates and distorted octahedral structure by Cu(II) complex. Cyclic voltammetry measurement analysed for Cu(II) complex shows a pair of cathodic and anodic peak potentials at 0.45 mV and 0.06 mV, suggesting the Cu(II)/Cu(I) couple and a quasi-reversible one electron transfer process is confirmed by the peak-to-peak separation value of $\Delta Ep = 0.39$ mV. Thermal stability of the synthesized compounds is ascertained from thermal studies which also confirm the presence of lattice and coordinated water molecules of hydration. The general formula for the composition of complexes is $[ML(CH_3COO)(H_2O)_2]. nH_2O$, in which M is Co(II), Ni(II), Cu(II), Zn(II) metal ion, L is the synthesized Schiff base, and n may be 1 or 2.

The *in vitro* antimicrobial result illustrates that coordination complexes of **L** are biologically more active towards bacteria than fungi. Cu(II) complex shows remarkable activity against *E. coli*. The activities towards bacterial and fungal species of the coordination complexes are greater than those of the **L**, which confirms that complexation with metal improves the reactivity. The Cu(II) complex of the study reveals greater superoxide activity with lowest IC_{50} value (14.2 mM) compared with Co(II), Ni(II) and Zn(II) complexes. The DNA is completely cleaved by Cu(II) and Zn(II) complex whereas Co(II), and Ni(II) complexes partially cleave the DNA. The metal complexes and **L** show better inhibitory resulton the propagation of LBir2754 cells. Among them, Cu(II) complex reveals better inhibitory activity on magnification of LBir2754 cells compared to the Co(II), Ni(II) and Zn(II) coordination complex and free **L**. The findings support the view that the synthesized compounds can be used as promising candidates for drug formulation and development owing to their diversity of bioactivities.

References

[1] Christiana XZ, Stephen JL (2003) New metal complexes as potential therapeutics. Current Opinion in Chemical Biology 2003, 7:481–489, DOI 10.1016/S1367-5931(03)00081-4.

[2] Anmol Singh , Pranjit Barman (2021) Recent Advances in Schiff Base Ruthenium Metal

Complexes: Synthesis and Applications. Topics in Current Chemistry. https://doi.org/10.1007/s41061-021-00342-w.

[3] Sakthivel A, Jeyasubramanian K , Thangagiri B, Dhaveethu Raja J (2020), Recent advances in Schiff base metal complexes derived from 4-amoniantipyrine derivatives and their potential applications, Journal of Molecular Structure. doi: https://doi.org/10.1016/j.molstruc.2020.128885.

[4] Ibtihal KK, Fawzi YW, Ghusoon JA **(**2019). Synthesis, Characterization and biological activity of Some Transition Metal Complexes with New Schiff Base Ligand Type (NNO) Derivative from Benzoin, Journal of Pharmaceutical Sciences and Research . 11. 119-124.

[5] Thahira BSA. Ravoof, Karen AC, Ibrahim M, Tahir M, Andrew RC, Akbar Ali M (2007) Synthesis, characterization and bioactivity of mixed-ligand Cu(II) complexes containing Schiff bases derived from S-benzyldithiocarbazate and saccharinate ligand and the X-ray crystal structure of the copper-saccharinate complex containingS-benzyl-b-N-(acetylpyrid-2-yl)methylenedithiocarbazate, Polyhedron, doi:10.1016/j.poly.2006.03.007.

[6] Tehrani KHME, Hashemi M, Hassan M, Kobarfard F, Mohebbi S (2015) Synthesis and antibacterial activity of schiff bases of 5-substituted isatins, Chinese Chemical Letters. http://dx.doi.org/10.1016/j.cclet.2015.10.027.

[7] Abu-Dief AM, Mohamed IMA (2015) A review on versatile applications of transition metal complexes incorporating Schiff bases, Beni-Suef University Journal of Applied Science doi: 10.1016/j.bjbas.2015.05.004.

[8] Rehab A, Barbara K, Nora A, Thomas V, Aida El-Ansary (2010) Antibacterial effect of some benzopyrone derivatives, European Journal of Medicinal Chemistry, doi:10.1016/j.ejmech.2009.10.001.

[9] Marianne F, Krishan K1, Anthony B (2016). Antibiotic resistance, Journal of Infection and Public Health, http://dx.doi.org/10.1016/j.jiph.2016.08.007.

[10] Laura FM, Bo Aronsson, Chris M, Inge CG, Anthony DS, Dominique LM, Otto C (2011) Critical shortage of new antibiotics in development against multidrug-resistant bacteria—Time to react is now, Drug Resistance Updates, doi:10.1016/j.drup.2011.02.003.

[11] Vogel AI (1978) A Textbook of Quantitative Inorganic Analysis Including Elementary Instrumental Analysis. Longman. London.

[12] Methods for Anti-Microbial Dilution and Disk Susceptibility Testing of Infrequently Isolated or Fastidious Bacteria; Approved Guideline Document M45-A (1999) National Committee for Clinical Laboratory Standrd. NCCLS. Villanova PA USA.

[13] Halli MB, Sumathi RB (2012) Synthesis, spectroscopic, antimicrobial and DNA cleavage studies of new Co(II),Ni(II), Cu(II), Cd(II), Zn(II) and Hg(II) complexes with naphthofuran-2-carbohydrazide Schiff base. Journal of Molecular Structure. http://dx.doi.org/10.1016/j.molstruc.2012.05.003

[14] Patel RN, Patel DK, Sondhiya VP, Shukla KK, Singh Y, Kumar A (2013) Synthesis, crystal structure and superoxide dismutase activity of two new bis(μ-acetato/μ-nitrato) bridged copper(II) complexes with N ’-[phenyl(pyridin-2-yl)methylidene]benzohydrazone. Inorganica Chimica Acta. http://dx.doi.org/10.1016/j.ica.2013.05.024

[15] Mosmann T (1983) Rapid Colorimetric Assay for Cellular Growth and Survival:Application to

Proliferation & Cytotoxicity Assays, Journal of Immunological Methods. 65 :55-63

[16] Monks A, Scudiero D, Skehan P, Shoemaker R, Paull K, Vistica D, Hose C, Langley J, Cronise P, Vaigro-Wolff A, Gray-Goodrich M, Campbell H, Mayo J, Boyd M (1991) Feasibility of a High-Flux Anticancer Drug Screen Using a Diverse Panel of CulturedHuman Tumor Cell Lines. J Natl Cancer Inst 83:757-766

[17] Justin Dhanaraj C, JebapriyaM (2020) Metal schiff base complexes of tridentate antipyrine based ligand: Synthesis, spectral characterisation, image analysis and biological Studies. Journal of Molecular Structure. https://doi.org/10.1016/j.molstruc.2020.128596.

[18] Lever, ABP 1984, 'Inorganic Electronic Spectroscopy'. second ed, Amsterdam ; Elsevier , New York

[19] Moamen SR, Ibrahim ME, Zeinab MA & Samir E (2009) 'Bivalent transition metal complexes of coumarin-3-yl thiosemicarbazone derivatives: Spectroscopic, antibacterial activity and thermogravimetric studies'. Journal of Molecular Structure, vol. 920, pp. 149-162.

[20] Banerjea, D (1993) Coordination Chemistry, Tata McGraw-Hill Pub, New Delhi

[21] Hosny M.El-Tabl, Fathy A. El-Saied, Mohamed I. Ayad, Manganese(II), Iron(III), Cobalt(II), Nickel(II), Copper(II), Zinc(II), And Uranyl(VI) Complexes Of N-(4-Formylantipyrine)Benzothiazol-2-ylacetohydrazide,Synthesis and Reactivity in Inorganic and Metal-Organic Chemistry, 32(2002),1245-1262 ,http://dx.doi.org/10.1081/SIM-120014301.

[22] Nagesh, GY, Mahendra Raj K, Mruthyunjayaswamy BHM. (2014) Synthesis, characterization, thermal study and biological evaluation of Cu(II), Co(II), Ni(II) and Zn(II) complexes of Schiff base ligand containing thiazole moiety, Journal of Molecular Structure, doi: http://dx.doi.org/10.1016/j.molstruc. 2014.09.013

[23] Dovinova I, Paulıkova H, Raukoc R. Hunakova L, Hanusovska E , Tibenska E (2002) Main targets of tetraaza macrocyclic copper complex on L1210 murine leukemia cells. Toxicology in Vitro. 16: 491–498

[24] Tisato F, Marzano C, Porchia M, Pellei M, Santini C (2010) Copper in Diseases and Treatments, and Copper-Based Anticancer Strategies. Medicinal Research Reviews. http://DOI 10.1002/med.20174.